Efficacy of Continued Fraction Expansion technique in the approximation of fractional order systems

Original Scientific Paper

Nitisha Shrivastava*

Ajay Kumar Garg Engineering College,
Department of Electrical and Electronics Engineering, Ghaziabad, Uttar Pradesh, India, 201015
nitishashrivastav@gmail.com

Arjun Baliyan

Jamia Millia Islamia
Department of Electrical Engineering, New Delhi, India, 110025
arjunbaliyaneee@gmail.com

*Corresponding author

Abstract – At a macroscopic level derivatives and integrals are the usual mathematical tools to model real time processes and to perform the basic control and signal processing actions. However, the analysis, design, synthesis and implementation of fractional order differentiator and integrator is a difficult task because of its irrational behaviour. Therefore, for mathematical evaluation of any fractional order system, conversion to its approximate integer order equivalent is essential. In this paper approximated integer order models of fractional differentiator and integrator are developed using the continued fraction expansion technique. A continued fraction is an expression obtained through an iterative process. For any iteration to terminate, a finite numerical value is assigned, which in this paper is equal to the number of frequency points within the desired frequency band. It includes both the lower and upper limit values. A set of coefficients are obtained by finding the gains of the fractional term at respective frequencies and thereby applying the recursive formula. The coefficients thus obtained are substituted in the expression of continued fraction which results in a polynomial function of finite order. The developed models can be directly applied for analysis and realization of fractional order systems. The models are developed for fractional terms 0.1 to 0.9 in steps of 0.1, and also for 0.25 and 0.75. A detailed discussion on the sensitivity analysis is presented, which includes the influence of variable parameters on the accuracy and length of the order. Simulations have been performed in MATLAB. A comparison with both, the ideal values and also with existing methods is performed and tabulated to validate the correctness of the developed models both in terms of accuracy and integer order of the model. It shows that the Matsuda method yield very good results both in terms of magnitude and phase. And, is most suitable for linear phase circuits. Also, the proposed models can be directly used for the realization of customized fractional order Proportional Integral (PI), Proportional-Derivative (PD) and PID controllers. To establish the correctness of CFE based technique for hardware realization, the integer order approximated model of one-tenth and seven-tenth differentiator is decomposed to obtain the circuit parameters resistor (R) and capacitor (C). Then its implementation in OrCAD Capture CIS is performed. It can be seen that the results of realization closely match the actual response.

1. INTRODUCTION

In recent years, researches have been able to explore many potential applications of fractional calculus in science, engineering and business administration [1-7]. It has also been shown that modeling and controlling many financial, biological, chemical, physical, electri-cal and control phenomena is better done using fractional order calculus [8-10]. Some physical phenomena which show fractional behaviour are; spectral densities of music, viscoelasticity (modelling of cement, gels, polymers), cardiac rhythm, diffusion in plasmas, transport of substances by water in soil, muscle activities, flexible transmission lines, path planning and tracking

for a mobile robot, heat diffusion in the soil, relaxation behaviour of polarized impedances in dielectrics and interfaces and hydraulic actuator.

In order that richness of the dynamic features exhibited by a system or process be properly modified, we need a model of the system, tools for its analysis, ways to specify the required behaviour, methods to design the controller, and techniques to implement them. Since the usual tools to model dynamic systems at a macroscopic level are integrals and derivatives, the algorithms that implement the controllers are mainly composed of such tools. Also, the basic control actions are proportional, derivative and integral. It is quite natural to conclude that by introducing more specific control actions and mathematical substitutes of the form s^α and $1/s^\alpha$, $(0 < \alpha < 1)$ we could achieve more satisfactory compromises between positive and negative effects and combining the actions we could develop more powerful and flexible design methods to satisfy the controlled system specifications [11-15]. In systems theory the analysis of dynamical behaviour is often made by means of transfer functions. The physical systems which exhibit fractional order (f-o) dynamic behaviour are described by f-o transfer functions in the s-domain. The simple form of a f-o transfer function is $F(s)=s^{\pm\alpha}$ $(0 < \alpha < 1)$. The form s^α is continuous time (c-t) f-o differentiator and the form $s^{-\alpha}$ is c-t f-o integrator. To implement transfer functions of this form is not easy, due to its infinite dimensional nature. Therefore, for implementation, it is required to convert fractional functions into integer order functions using different approximation techniques [16-24]. These techniques which are available in literature are based on rational approximations in the frequency domain developed to approximate the arbitrary order with low level of error and wide bandwidth, such as Oustaloup's [16], refined Oustaloup's [17], Charef's [18], Carlson's [19, 20], Matsuda's [21], etc. Both Oustaloup and refined Oustaloup methods are based on pole and zero recursion and are useful where a frequency band of interest is set initially. Also the desired order of the developed model can be chosen a priori. Charef method is also based on interlacing of pole-zero technique, but in this technique the desired order of the developed model cannot be chosen a priori. And moreover, the order of the developed model depends on the fractional order α. The Carlson method is based on Newton iterative process. Similar to Charef method here also the order of the developed model depends on fractional order α and is not uniform for all values of α. In Matsuda method the approximation is obtained using Continued fraction expansion technique and the frequency band as well as the order of the approximated model is set initially. The approximation of fractional differentiator $s^{0.5}$ using different methods is summarized in a survey paper [25]. There are many more applications of fractional order calculus. For example, a synthesis methodology of fractional-order chaotic systems was discussed in [26]. The analysis and analog design of fractional-order charge/flux controlled memristor emulators of incremental/decremental type was described in [27]. In [10, 28, 29] the analog design of fraction-

al-order proportional-integral-derivative controllers was reported. The fractional-order lead/lag compensator was investigated in [30, 31]. The design of double exponent fractional-order filters and power law filters were investigated in [32, 33], respectively, and so on. The dynamic analysis, and subsequently the hardware implementation and realization of such systems can be performed after representing them with finite number of poles and zeros. Usually, hardware implementation of finite order transfer functions is done easily using electronic components/devices. Therefore, in order to study the dynamical behaviour, and for hardware realization purposes, the integer order approximation of the f-o system is required.

Here, the authors have proposed rational approximations of fractional order operator s^α for all values of α in the range (-1 to 1) upto one decimal place and for $\alpha = \pm\frac{1}{4}$ & $\pm\frac{3}{4}$. This forms one of the major contributions of the paper. While analysing fractional order systems, if the integer order approximation of the different fractional orders is readily available, then the fractional order transfer function is converted to its integer order equivalent by merely substituting the approximations of the fractional orders. The resulting transfer function then best approximates the original fractional order system. The Matsuda approximation technique has been utilized for this purpose. Though, this technique is well established, the effect of variation of the parameters used to develop the approximation has not been considered yet. So, another major contribution of the paper is to highlight the variation in frequency response of the approximated integer order models of fractional operator by varying its parameters. The findings are as follows: In Matsuda method there are two important parameters to be selected. One is the number of frequency points (n) and the other is the frequency range for which the developed model is to be used. The relation between differentiator and integrator is that they are inversely proportional to each other and this concept is true for most of the models developed using the different approximation techniques. But this is not applicable to all the models developed by Matsuda method.

The approximate fractional order derivatives obtained as ratio of polynomials in the Laplace domain can be implemented using analog and digital electronics. However, in both cases the exactness depends on the approximation to solve the fractional order function. The correctness of the circuit is therefore dependent on the numerical method and approximated Laplace model used for synthesis. The Field Programmable Analog Array (FPAA) and Field Programmable Gate Array (FPGA) can be used for fast verification and prototyping of fractional order dynamical systems. The circuit whose output displays the behaviour of an irrational function is known as fractional order element (FOE) or fractance device in literature [34-39]. The analog realization with different topologies viz., ladder network, nested ladders, first order RC filters, CMOS OTA based filters have been presented in [40, 41]. The authors in [42] present implementation of resistor less fractional order filters. A review of all the recent developments on the realization of frac-

tance devices can be found in [43]. A comparative study of discrete component realization is given in [44]. The FPGA realization of fractional order chaotic systems is explained in [45, 46]. The drawback in FPGA implementation is that the hardware resources are dependent on the length of the digital word that is used, and this can degrade the desired response due to the finite number of bits to perform computer arithmetic. Therefore implementation with analog electronics using FPAA is good alternative to achieve desired accuracy as presented in [47]. This paper demonstrates a generalized design procedure to develop a passive element R-C structure of fractional order differentiator. As an example, two fractional order differentiators of powers 0.7 (seven-tenth differentiator) and 0.1 (one-tenth differentiator) are simulated using the circuit simulator OrCAD Capture PSpice. A general formula for magnitude and frequency scaling is also presented. The magnitude and phase plots are discussed.

The section wise sequence is as follows: Introduction is covered in Section I. Matsuda method is explained in Section II. In this section integer order models of fractional order differentiator developed using the Continued Fraction Expansion (CFE) formula is listed. Performance and simulation results are discussed in Section III. Seven-tenth and one-tenth differentiator is realized using OrCAD Capture CIS and is presented in Section IV. The conclusion of the paper is in Section V.

2. METHOD

In this section the mathematical steps involved to develop the approximated integer order (AIO) models of fractional differentiators and integrators of order α, ($\alpha \in$ ([± 0.1, ± 0.9] *in steps of* 0.1 *and* $\pm 1/4$, $\pm 3/4$)) based on CFE technique are discussed. This method is popularly known as Matsuda method among the fractional community.

The fractional order (f-o) operator is given as [22]

$$F(s) = s^{\pm \alpha}; (0 < \alpha < 1) \quad (1)$$

The f-o differentiator (FOD) is defined as [22]

$$G(s) = s^{\alpha}; (0 < \alpha < 1) \quad (2)$$

The f-o integrator (FOI) is defined as [22]

$$H(s) = s^{-\alpha}; (0 < \alpha < 1) \quad (3)$$

In Matsuda method, the approximated integer order transfer functions of the f-o system are obtained by the use of CFE [21]. For the fractional order α, there are two parameters to be set before applying the formula of continued fraction expansion as given in Eqn. (4). The two parameters are: number of frequency points (n) and the specific Frequency Band (FB) in which the approximation is to developed. ω_i's are the numerical values of the frequency points. A detailed explanation of the frequency band and frequency points is given in section 3.1.1. a_i's are the set of coefficients which are obtained using Eqn. (5). The f-o operator in (1) can be replaced by its equivalent integer order function given as [21, 22]

$$F'(s) = a_1 + \cfrac{s - \omega_1}{a_2 + \cfrac{s - \omega_2}{a_3 + \cfrac{s - \omega_3}{a_4 + \dots}}} \quad (4)$$

In Eqn. (4) a_i's are the set of coefficients at different frequencies ωi ($1 \le i \le n$), which are defined within a desired FB [21, 22].

$$a_i = \frac{\omega_i - \omega_{i-1}}{q_{i-1}(\omega_i) - q_{i-1}(\omega_{i-1})}; \text{ for } i = 2,3,\dots,n \quad (5)$$

where $q_1(\omega_i) = |F(j\omega_i)|$ for $i = 1,2,3,\dots,n$ $|F(j\omega_i)|$ are the gains at respective frequencies.

The expression to find gain $|F(j\omega_i)|$ at a specific frequency ω_i is equal to $\pm(\alpha) \times 20 \log \omega_i$

Rest of the q's ($q_2, q_3 \dots, q_n$) are obtained using the recursive formulae [21, 22]

$$q_2(\omega_i) = \frac{\omega_i - \omega_1}{q_1(\omega_i) - q_1(\omega_1)} \text{ for } i = 2,3,\dots,n$$

$$q_3(\omega_i) = \frac{\omega_i - \omega_2}{q_2(\omega_i) - q_2(\omega_2)} \text{ for } i = 3,4,\dots,n$$

$$\vdots$$

$$q_n(\omega_i) = \frac{\omega_i - \omega_{n-1}}{q_{n-1}(\omega_i) - q_{n-1}(\omega_{n-1})} \text{ for } i = n$$

Using Eqn. (4), the AIO models of f-o differentiators and integrators are derived and analyzed in the coming subsections.

The analysis of f-o differentiators based on Matsuda method is performed for all orders of α with FB [10^{-2}, 10^2] and $n = 9$. The frequency points within this band are set as [0.01, 0.0316, 0.1, 0.3162, 1, 3.1623, 10, 31.6228, 100]. Using this data, the AIO transfer functions for the FOD s^α, ($\alpha \in$ ([0.1:0.1:0.9] *and* 1/4, 3/4)) are derived and given in Table 1.

Table 1. AIO transfer function of FOD s^α, ($\alpha \in$ ([0.1:0.1:0.9] and 1/4, 3/4))using Matsuda method in FB

s^α	$G\_m atsuda(s)$
$s^{0.1}$	1.828((s+52.78)(s+3.143)(s+0.2456)(s+0.01342)/ (s+74.5)(s+4.071)(s+0.3181)(s+0.01894))
$s^{0.2}$	3.3572((s+44.96)(s+2.766)(s+0.2155)(s+0.01111)/ (s+89.98)(s+4.64)(s+0.3615)(s+0.02224))
$s^{0.3}$	6.2275((s+38.54)(s+2.435)(s+0.1887)(s+0.009063)/ (s+110.3)(s+5.298)(s+0.4106)(s+0.02594))
$s^{0.4}$	11.7439((s+33.2)(s+2.145)(s+0.165)(s+0.007245)/ (s+138)(s+6.06)(s+0.4661)(s+0.03011))
$s^{0.5}$	22.7203((s+28.72)(s+1.89)(s+0.1439)(s+0.005634)/ (s+177.5)(s+6.948)(s+0.5291)(s+0.03481))
$s^{0.6}$	47.7342((s+24.93)(s+1.665)(s+0.1252)(s+0.004207)/ (s+237.7)(s+7.987)(s+0.6006)(s+0.0401))
$s^{0.7}$	98.224((s+21.7)(s+1.467)(s+0.1085)(s+0.002945)/ (s+339.5)(s+9.211)(s+0.6817)(s+0.04607))
$s^{0.8}$	237.755((s+18.94)(s+1.292)(s+0.09376)(s+0.001833)/ (s+545.5)(s+10.66)(s+0.7741)(s+0.05278))
$s^{0.9}$	769.99((s+16.56)(s+1.137)(s+0.08061)(s+0.0008552)/ (s+1169)(s+12.4)(s+0.8795)(s+0.06036))
$s^{0.25}$	4.565((s+41.6)(s+2.595)(s+0.2017)(s+0.01006)/ (s+99.42)(s+4.957)(s+0.3853)(s+0.02403))
$s^{0.75}$	149.6819((s+20.27)(s+1.376)(s+0.1009)(s+0.002371)/ (s+421.6)(s+9.906)(s+0.7264)(s+0.04932))

3. SIMULATION RESULTS

This section presents frequency response analysis of the approximated models. As examples magnitude and phase error plots of $s^{0.1}$, $s^{0.7}$ and $s^{0.25}$ are shown in Section 3.1. In section 3.1.1 the effect of variation of n and FB on FOD response is discussed and results analyzed. Similarly, magnitude and phase error plots of $1/s^{0.4}$, $1/s^{0.8}$ and $1/s^{0.75}$ are shown in Section 3.2 and the effect of variation of n and FB on FOI response is discussed in Section 3.2.1.

The outcome of the analysis is summarized highlighting the limitations and advantages of the proposed method. The Matsuda method based FOD models developed in this paper are compared with models developed using four other rational approximation techniques. The results of the comparison are tabulated in Section 3.3.

The comparison has three components: one is the maximum magnitude error in dB and second is the maximum phase error in degree with respect to their ideal values, and third is the order of the approximated model.

3.1. MATSUDA METHOD BASED FOD

The magnitude and phase plots of one-tenth differentiator $s^{0.1}$ (model given in Table 1) is shown in Fig. 1. Also shown is the ideal continuous bode of f-o differentiator $s^{0.1}$ for comparison. The magnitude and phase responses of Matsuda based one-tenth differentiator closely matches the continuous bode in the defined FB $[10^{-2}, 10^2]$.
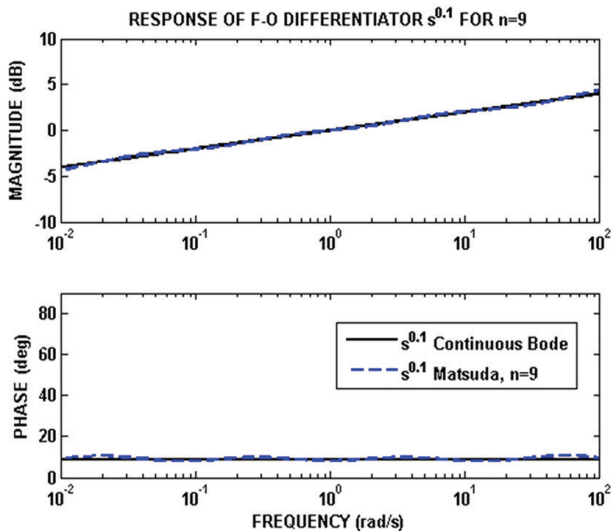
Fig. 1. Frequency Response of Matsuda based one-tenth differentiator $s^{0.1}$ in FB $[10^{-2}, 10^2]$, $n = 9$

Figs 2 and 3 show the magnitude and phase plots of Matsuda based f-o differentiators $s^{0.7}$ and $s^{0.25}$ (models given in Table 1) compared with their respective ideal continuous bode counterparts. It is seen that the responses closely match the ideal responses.
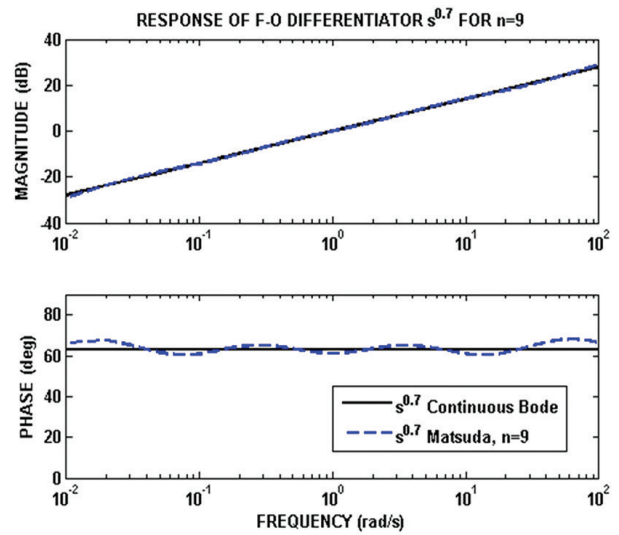
Fig. 2. Frequency Response of Matsuda based seven-tenth differentiator $s^{0.7}$ in FB $[10^{-2}, 10^2]$, $n = 9$
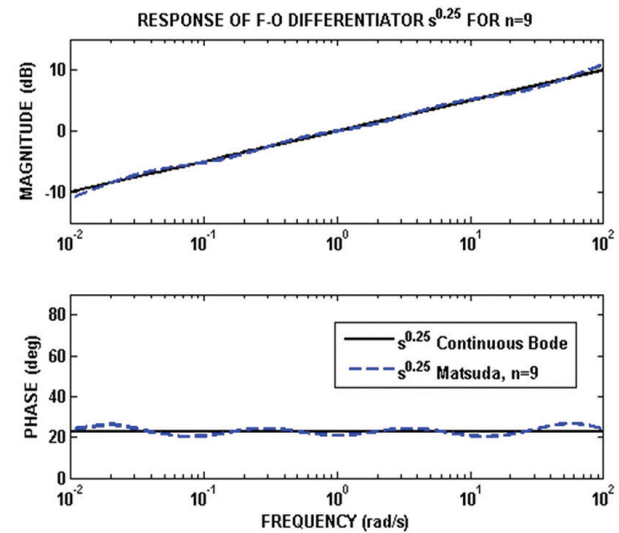
Fig. 3. Frequency Response of Matsuda based one-fourth differentiator $s^{0.25}$ in FB $[10^{-2}, 10^2]$, $n = 9$

3.1.1. Effect of Variation of n and FB on FOD Response

Matsuda method, the effect of variation of the two parameters - the specific FB and the number of frequency points within it, on the response of the AIO transfer function of FOD is studied and results analyzed.

Case 1: For this purpose, n is set as 9 and the AIO transfer function for one-tenth differentiator $s^{0.1}$ is

$$G_{0.1\_matsuda1}(s) = \frac{1.828s^4 + 102.7s^3 + 329.8s^2 + 78.9s + 0.9996}{s^4 + 78.91s^3 + 329.8s^2 + 102.7s + 1.827} \quad (6)$$

Case 2: If the FB is changed to $[10^{-2}, 10^2]$, the frequency points change [1, 1.7783, 3.1623, 5.6234, 10, 17.7828, 31.6228, 56.2341, 100] and keeping n same, the AIO for $s^{0.1}$ becomes

$$G_{0.1\_matsuda2}(s) = \frac{1.6s^4 + 33.29s^3 + 77.75s^2 + 27.43s + 1}{s^4 + 27.43s^3 + 77.75s^2 + 33.29s + 1.6} \quad (7)$$

We observe that the order of the transfer function remains same but the position of poles and zeros vary.

Case 3: Now, keeping FB as in Case 1 and varying $n = 13$ with frequency points set as [0.01, 0.0215, 0.0464, 0.1, 0.2154, 0.4642, 1, 2.1544, 4.6416, 10, 21.5443, 46.4159, 100], the approximated transfer function for $s^{0.1}$ is

$$G_{0.1\_matsuda3}(s) = \left(\frac{\begin{array}{c}1.946s^6+268.2s^5+3779s^4+8363s^3\\+3162s^2+183.8s+0.9988\end{array}}{\begin{array}{c}s^6+183.9s^5+3163s^4+8363s^3\\+3778s^2+268s+1.944\end{array}} \right) \quad (8)$$

From Eqn. (8) it is clear that when n is increased, the order of the transfer function increases.

Fig. 4 shows the position of poles and zeros for the three cases. Generalizing, it can be inferred that for different FBs, if n remains unchanged, only the position of poles and zeros vary; but the order remains same. And if n is varied, the order of the approximated transfer function also changes. Further, if n is increased, the plots exhibit better matching with the ideal continuous time (c-t) domain f-o differentiator. Analysis can also be performed for different FBs and different n.

The set of frequencies generated in the FB [10^0, 10^2] and various n are listed in Table 2. Table 3 shows the set of frequency points for $n= 9$ in different FBs.
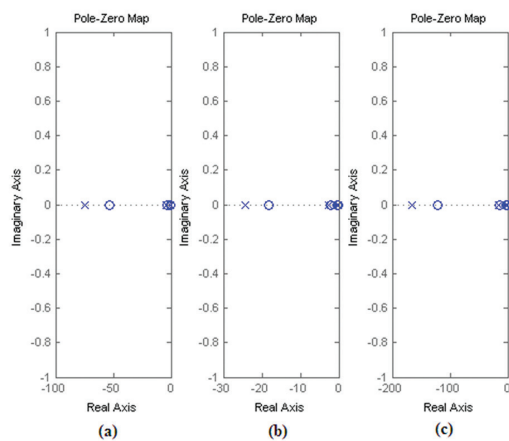
Fig. 4. Pole-zero maps of Matsuda based $s^{0.1}$ for different FBs & n (a) [10^{-2},10^2], $n = 9$ (b) [$10^{0.1}$, 10^2], $n = 9$ (c) [10^{-2},10^2], $n =13$

Table 2. Matsuda method: Set of frequency points for different n in the FB [10^{-2}, 10^2]

n	Frequency points
3	0.01, 1, 100
5	0.01, 0.1, 1, 10, 100
7	0.01, 0.0464, 0.2154, 1, 4.6416, 21.5443, 100
9	0.01, 0.0316, 0.1, 0.3162, 1, 3.1623, 10, 31.6228, 100
11	0.01, 0.0251, 0.0631, 0.1585, 0.3981, 1, 2.5119, 6.3096, 15.8489, 39.8107, 100
13	0.01, 0.0215, 0.0464, 0.1, 0.2154, 0.4642, 1, 2.1544, 4.6416, 10, 21.5443, 46.4159, 100
15	0.01, 0.0193, 0.0373, 0.0720, 0.1389, 0.2683, 0.5179, 1, 1.9307, 3.7276, 7.1969, 13.8950, 26.8270, 51.7947, 100
17	0.01, 0.0178, 0.0316, 0.0562, 0.1, 0.1778, 0.3162, 0.5623, 1, 1.7783, 3.1623, 5.6234, 10, 17.7828, 31.6228, 56.2341, 100

FB	Group of frequencies for $n=9$
[10^0, 10^2]	1, 1.7783, 3.1623, 5.6234, 10, 17.7828, 31.6228, 56.2341, 100
[10^{-2}, 10^2]	0.01, 0.0316, 0.1, 0.3162, 1, 3.1623, 10, 31.6228, 100
[10^{-3}, 10^3]	0.001, 0.0056, 0.0316, 0.1778, 1, 5.6234, 31.6228, 177.8279, 1000
[10^{-1}, 10^5]	0.1, 0.5623, 3.1622, 17.7828, 100, 562.3413, 3162.2776, 17782.7941, 100000
[10^{-1}, 10^1]	0.1, 0.1778, 0.3162, 0.5623, 1, 1.7783, 3.1623, 5.6234, 10
[10^3, 10^5]	1000, 1778.2794, 3162.2776, 5623.4132, 10000, 17782.7941, 31622.7766, 56234.1325, 100000

Table 3. Matsuda method: Group of frequencies for different FBs, for $n=9$

To study the effect of variation of n, the response of one-tenth differentiator s^0.1 has been plotted with FB [10^{-2}, 10^2] with $n = 7$, 9, 11, 13 and is shown in Fig. 5. The corresponding magnitude and phase errors are shown in Fig. 6.
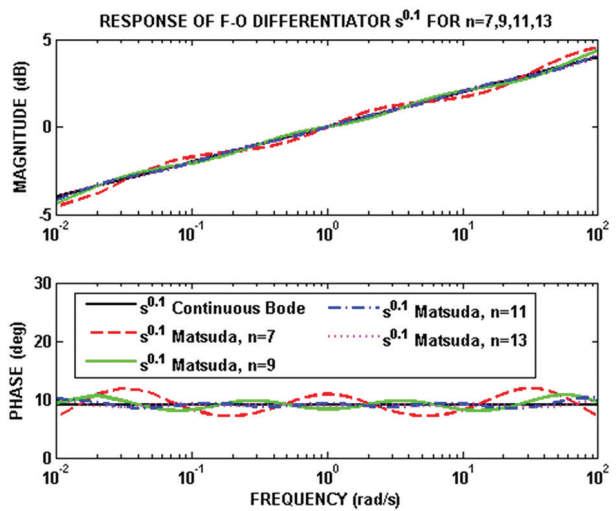
Fig. 5. Frequency Response of Matsuda based one-tenth differentiator $s^{0.1}$ in FB [10^{-2}, 10^2], $n = 7,9,11,13$
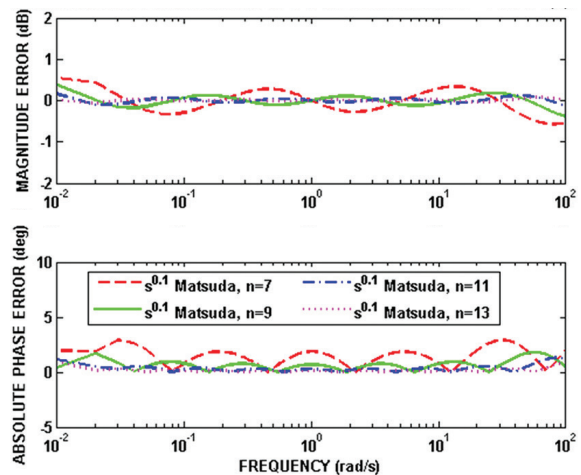
Fig. 6. Magnitude and phase errors of Matsuda based one-tenth differentiator $s^{0.1}$ in FB [10^{-2}, 10^2], $n = 7,9,11,13$

From the frequency response and error plots, we see that as the choice of number of frequency points increases the response matches more closely to the ideal c-t domain one-tenth differentiator. For the entire FB [10^{-2}, 10^2], the maximum magnitude error is less than 0.5 dB "*for*" $n \geq 9$ and the flatness of the phase diagram is obtained for $n=13$ which finds application in linear phase circuits. It is also observed that the magnitude error of the approximant is least at the chosen frequency points.

As the choice of the number of frequency points increases, the order of the AIO transfer function also increases and accuracy towards the actual value is attained.

An important point worth mentioning here is that the order of the approximated transfer function does not depend on the order of the fractional operator.

Another important inference is that proper approximated models are obtained only for odd values of n and the system is non-causal for even values of n. To illustrate this, let the number of poles be n_p and the number of zeros be n_z.

For odd value of n, $n_p = n_z = (n-1)/2$ ie. the numerator and denominator polynomials have the same order. For even value of n, $n_p = (n/2)-1$ and $n_z = n/2$ the numerator polynomial has order one higher than denominator polynomial. Since system is non-causal, further analysis has not been pursued for FODs. Table 4 lists the order of the AIO models obtained for different values of n.

Table 4. Order of Approximated transfer function of FOD s^α using Matsuda method for different values of n

n	3	5	7	9	11	13	15	17
Order of approximated integer order model	1	2	3	4	5	6	7	8

3.2. MATSUDA METHOD BASED FOI

The AIO transfer functions of the FOI in Eqn. (3) are obtained by directly inverting the transfer function of the models obtained in Section 2. This is due to the fact that the order of numerator and denominator polynomials is same in the models of Table 1. All the models thus obtained are stable.

Figures 7, 8 and 9 show the frequency responses of Matsuda based f-o integrator $1/s^{0.4}$,$1/s^{0.8}$ and $1/s^{0.75}$ respectively compared with their ideal continuous bode responses in the FB [10^{-2}, 10^2] and n set as 9. It is observed that the responses of the Matsuda based f-o integrator models closely match the ideal responses.

In Section 2 the AIO models of FOD were obtained only for odd values of n; the models being non-causal for even values of n. An important observation is that by inverting the models with even values of n, we could obtain transfer functions with order of the numerator one less than that of denominator. The order of the model developed for even values of n is $n/2$. Figs. 10, 11 and 12 show the frequency responses of Matsuda based f-o integrator $1/s^{0.1}$,$1/s^{0.3}$ and $1/s^{0.8}$ respectively compared

with their ideal continuous bode responses in the *FB* [10^{-2}, 10^2] and n set as 8. It is seen that the responses of these Matsuda based f-o integrator models for even values of n also closely match the ideal responses.
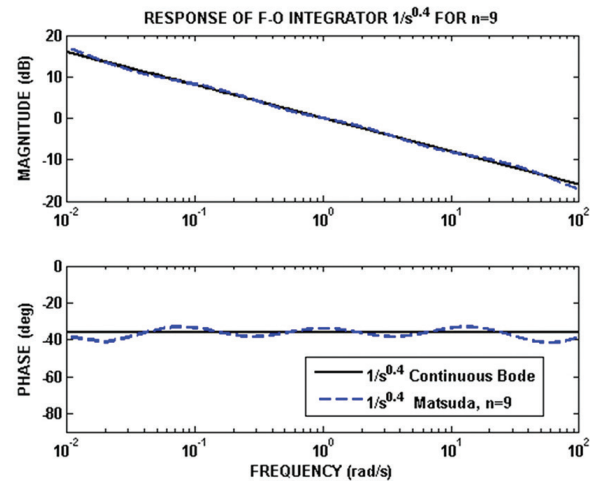
Fig. 7. Frequency Response of Matsuda based four-tenth integrator $1/s^{0.4}$ in FB [10^{-2}, 10^2], $n = 9$
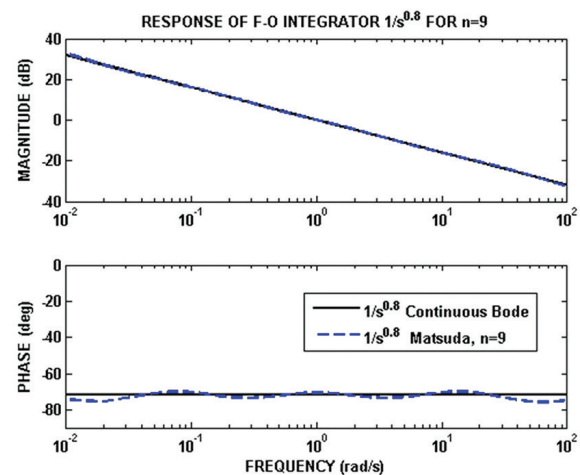
Fig. 8. Frequency Response of Matsuda based eight-tenth integrator $1/s^{0.8}$ in FB [10^{-2}, 10^2], $n = 9$
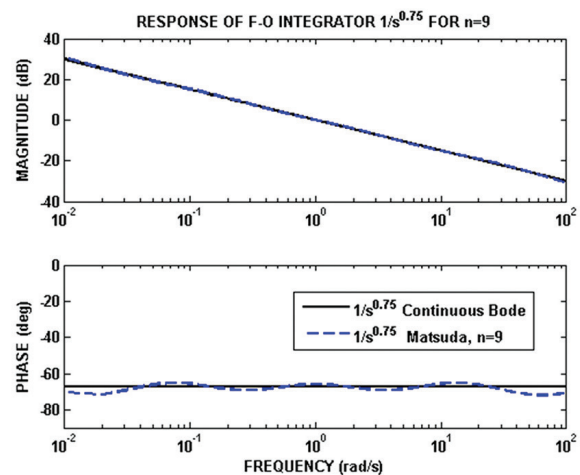
Fig. 9. Frequency Response of Matsuda based three-fourth integrator $1/s^{0.75}$ in FB [10^{-2}, 10^2], $n = 9$

International Journal of Electrical and Computer Engineering Systems
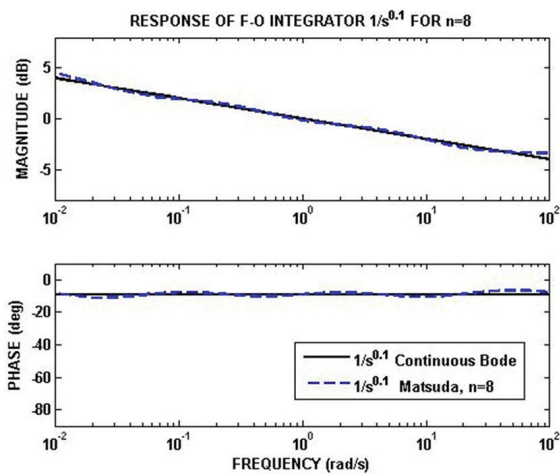
Fig. 10. Frequency Response of Matsuda based one-tenth integrator $1/s^{0.1}$ in FB [10^{-2}, 10^2], $n = 8$
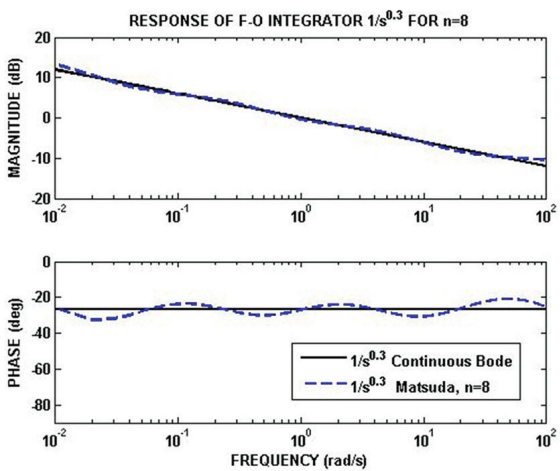
Fig. 11. Frequency Response of Matsuda based three-tenth integrator $1/s^{0.3}$ in FB [10^{-2}, 10^2], $n = 8$
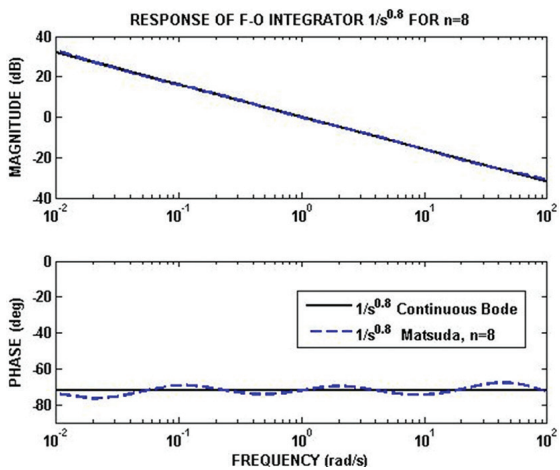
Fig. 12. Frequency Response of Matsuda based eight-tenth integrator $1/s^{0.8}$ in FB [10^{-2}, 10^2], $n = 8$

3.2.1. Effect of Variation of n and FB on FOI Response

Since FOI models are obtained directly by inverting the FOD models, the discussion presented in section 2 also holds true for FOI response.

To study the effect of variation of n, simulations have been performed for four-tenth integrator $1/s^{0.4}$ with different odd values of n and one-tenth integrator $1/s^{0.1}$ with different even values of n.

Fig. 13 shows the frequency response of approximated Matsuda based four-tenth integrator $1/s^{0.4}$ as compared to the c-t domain FOI for the *FB* [10^{-2}, 10^2], $n = 9$, 11, 13, 15 and their corresponding magnitude and phase error plots are shown in Fig. 14. It is seen that if n is increased, the response matches very closely to ideal c-t domain FOI $1/s^{0.4}$. The maximum magnitude error is less than 0.5 dB and the maximum phase error is less than 5° for $n \geq 11$. The maximum magnitude error is less than 0.1 dB for $n \geq 13$ and the phase response is flat for $n = 15$ in the FB [10^{-1}, 10^1]. The frequency response of Matsuda based one-tenth integrator $1/s^{0.1}$ in the FB [10^{-2}, 10^2]," for " $n = 6, 8, 10, 12$ is shown in Fig. 15.

The plot is compared with the ideal response of one-tenth integrator and it is seen that if n is increased, the response matches closely to ideal c-t domain FOI $1/s^{0.1}$. The corresponding magnitude and phase error plots are shown in Fig 16. It is seen that the maximum magnitude error is less than 0.3 dB for $n = 12$ and maximum phase error is less than 5° for $n = 6, 8, 10, 12$.
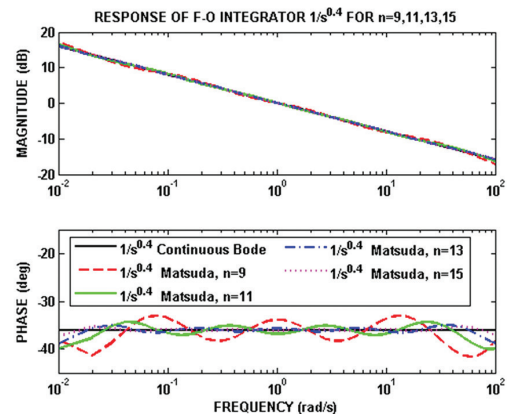
Fig. 13. Frequency Response of Matsuda based four-tenth integrator $1/s^{0.4}$ in FB [10^{-2}, 10^2], $n = 9$, 11, 13, 15
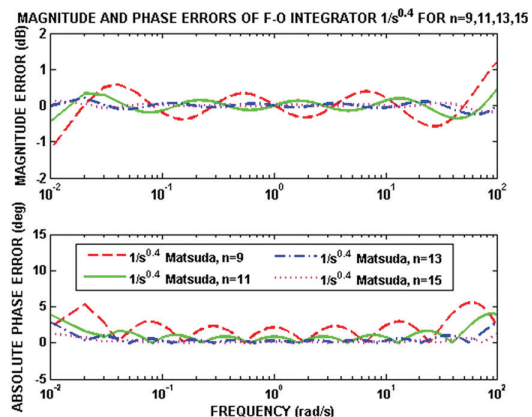
Fig. 14. Magnitude and phase errors of Matsuda based four-tenth integrator $1/s^{0.4}$ in FB [10^{-2}, 10^2], n = 9, 11,13,15
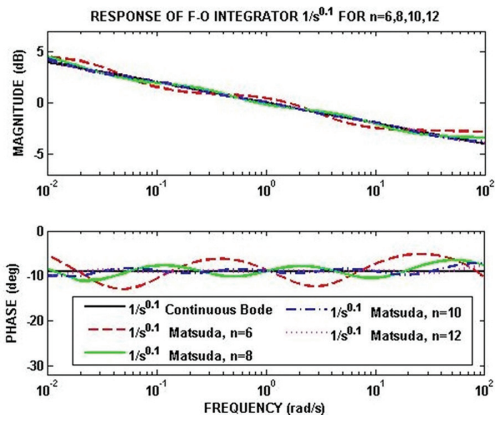
Fig. 15. Frequency Response of Matsuda based one-tenth integrator $1/s^{0.1}$ in FB [10^{-2}, 10^2], $n = 6, 8, 10, 12$
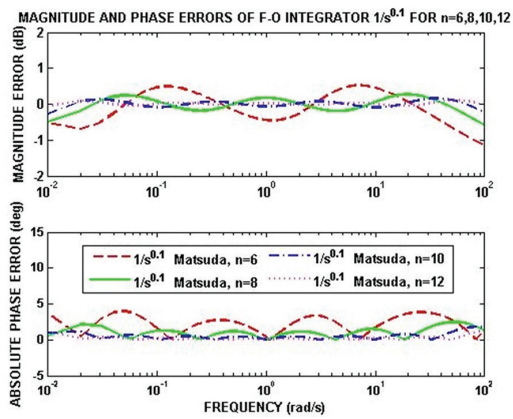
Fig. 16. Magnitude and phase errors of Matsuda based one-tenth integrator $1/s^{0.1}$ in FB [10^{-2}, 10^2], $n = 6, 8, 10, 12$

Simulations have been performed for FOD and FOIs for order α ($\alpha \in$ ([±0.1:±0.1:±0.9] and $\pm1/4$, $\pm3/4$)) in the FB [10^{-2}, 10^2] for different odd and even values of n using Matsuda method of approximation. Similar observations were noted. It is seen that accurate approximation is achieved for both magnitude and phase for higher values of n, specifically for $n \geq 13$.

3.3. COMPARATIVE STUDY

In this section, a comparative analysis of the FOD models developed in this paper is done with models developed using four other rational approximation techniques. These are Charef method, Carlson method, Oustaloup method and Modified Oustaloup method. The comparison is based on the frequency response of the models i.e. maximum magnitude and phase errors are compared as shown in Tables 5 and 6. Also order of the developed approximated models are mentioned in the comparison table as it is an important factor for realization purposes. Since the number of active/passive elements required for hardware implementation depends upon the order of the approximated model, a compact hardware can be made only with lesser number of components.

In Carlson method and Charef method there is no provision in the formula to select the desired order for which the approximation is to be developed [20, 39]. Only the desired frequency band can be chosen a priori. The order of the approximated model depends on the fractional order α. But in the Oustaloup method and Modified Oustaloup method both desired order and desired frequency band can be selected before applying the formula [16, 17]. This can also be seen from the Tables 5 and 6 that all the models developed by applying Matsuda, Oustaloup and modified Oustaloup methods have fixed orders, 4, 5 and 5 respectively. Whereas for the models based on Charef and Carlson methods the integer orders are not fixed. It depends on the value of α. Although we can the assign a parameter for desired order in Oustaloup and modified Oustaloup methods, but the order of the generated transfer function will always be an odd number [16, 17]. For comparison, the order of these models are chosen as 5, because the models having order 3 gave very poor results.
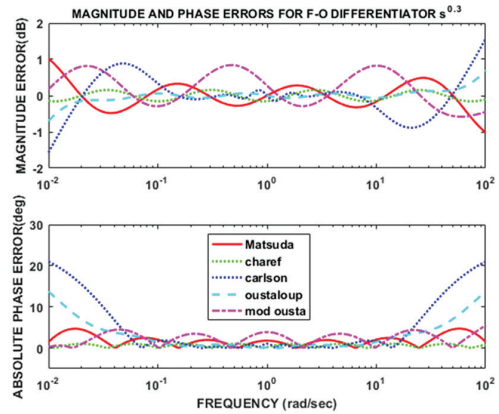
Fig. 17. Magnitude and phase errors of Matsuda, Charef, Carlson, Oustaloup and Modified Oustaloup based three-tenth differentiator $s^{0.3}$ in FB [10^{-2}, 10^2]
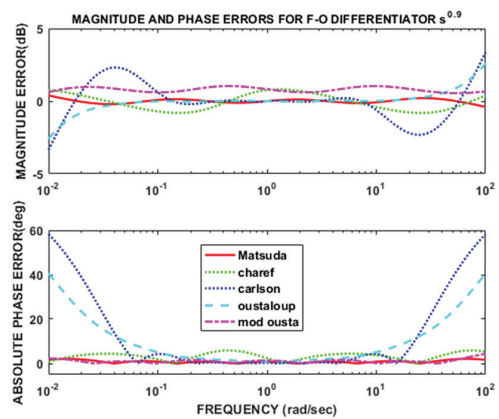
Fig. 18. Magnitude and phase errors of Matsuda, Charef, Carlson, Oustaloup and Modified Oustaloup based nine-tenth differentiator $s^{0.9}$ in FB [10^{-2}, 10^2]

As an example, the maximum magnitude and phase error plots is shown in Fig 17 for FOD $s^{0.3}$. The corresponding error values obtained after simulation is presented in Tables 5 and 6. It can be seen that maximum

magnitude error is least for Charef method which is 0.15 dB, and is 0.69 dB in Oustaloup method, 0.84 dB in Modified Oustaloup method, 1.02 dB in Matsuda method and 1.56 dB in Carlson method. The maximum phase error is 1.04°, 4.72°, 5.54°, 13.72° and 21.01° for models based on Charef, Matsuda, Modified Oustaloup, Oustaloup and Carlson methods respectively. Fig. 18 shows the maximum magnitude and phase error plots of FOD $s^{0.9}$ and its corresponding error values are tabulated in Tables 5 and 6. It can be seen that Matsuda based model has least maximum magnitude error of 0.39 dB. The maximum magnitude error for Charef, Modified Oustaloup, Oustaloup and Carlson methods are 0.81 dB, 1.03 dB, 2.58 db and 3.36 dB respectively. Also Matsuda based model has least maximum phase error of 2.08° and it is 4.39° and 5.85° for Modified Oustaloup and Charef based models respectively and is very high

for Oustaloup (40.57°) and Carlson (58.21°) method approximated models. Similarly, simulations have been performed for all FOD of order α ($\alpha \in$([0.1:0.1:0.9] and 1/4, 3/4)) in the FB [10^{-2}, 10^2] and results tabulated. It can be seen that order of Matsuda based models is 4, which is least among all the other methods. Also it can be seen that the accuracy of the proposed Matsuda based models is very good in comparison to Carlson, Oustaloup and Modified Oustaloup methods. Although Charef based models have lesser magnitude and phase errors but the order of the approximated models are very high which is not suitable for implementation purposes. Therefore Matsuda based models are both accurate and have least order among all other methods and are therefore most suitable for applications in linear phase circuits.

Table 5. Maximum Magnitude Error comparison between proposed FOD s^{α}, ($\alpha \in$([0.1:0.1:0.9] and 1/4, 3/4)) in the FB [10^{-2}, 10^2] with four different methods

s^{α}	Maximum Magnitude Error (in dB)				
	Matsuda Method (ALL order 4)	Charef Method	Carlson Method	Oustaloup Method (ALL order 5)	Modified Oustaloup Method (ALL order 5)
$s^{0.1}$	0.38	0.81 (Order 4)	0.54 (Order 12)	0.22	0.30
$s^{0.2}$	0.73	0.33 (Order 7)	1.02 (Order 7)	0.45	0.59
$s^{0.3}$	1.02	0.15 (Order 9)	1.56 (Order 19)	0.69	0.84
$s^{0.4}$	1.20	0.09 (Order 10)	2.04 (Order 14)	0.95	1.03
$s^{0.5}$	1.27	0.08 (Order 11)	1.32 (Order 4)	1.22	1.15
$s^{0.6}$	1.21	0.09 (Order 11)	1.86 (Order 16)	1.52	1.21
$s^{0.7}$	1.03	0.15 (Order 11)	2.34 (Order 11)	1.84	1.20
$s^{0.8}$	0.74	0.33 (Order 8)	2.88 (Order 23)	2.20	1.14
$s^{0.9}$	0.39	0.81 (Order 5)	3.36 (Order 18)	2.58	1.03
$s^{0.25}$	0.88	0.22 (Order 8)	1.21 (Order 6)	0.57	0.72
$s^{0.75}$	0.89	0.22 (Order 9)	2.53 (Order 10)	2.02	1.18

Table 6. Maximum Phase Error comparison between proposed FOD FOD s^{α}, ($\alpha \in$([0.1:0.1:0.9] and 1/4, 3/4)) in the FB [10^{-2}, 10^2] with four different methods

s^{α}	Maximum Phase Error (in degrees)				
	Matsuda Method (ALL order 4)	Charef Method	Carlson Method	Oustaloup Method (ALL order 5)	Modified Oustaloup Method (ALL order 5)
$s^{0.1}$	1.79	5.85 (Order 4)	7.06 (Order 12)	4.57	2.22
$s^{0.2}$	3.40	2.24 (Order 7)	13.95 (Order 7)	9.15	4.06
$s^{0.3}$	4.72	1.04 (Order 9)	21.01 (Order 19)	13.72	5.54
$s^{0.4}$	5.58	0.64 (Order 10)	27.90 (Order 14)	18.25	6.54
$s^{0.5}$	5.94	0.56 (Order 11)	30.31 (Order 4)	22.77	7.03
$s^{0.6}$	5.75	0.65 (Order 11)	37.38 (Order 16)	27.26	7.01
$s^{0.7}$	5.02	1.05 (Order 11)	44.26 (Order 11)	31.72	6.52
$s^{0.8}$	3.78	2.24 (Order 8)	51.32 (Order 23)	36.16	5.61
$s^{0.9}$	2.08	5.85 (Order 5)	58.21 (Order 18)	40.57	4.39
$s^{0.25}$	4.11	1.48 (Order 8)	17.25 (Order 6)	11.44	4.86
$s^{0.75}$	4.46	1.49 (Order 9)	47.56 (Order 10)	33.94	6.11

4. IMPLEMENTATION OF FOD

The proposed Matsuda method based fractional order differentiators listed in Table 1 are developed using the CFE formula given in Eqn. 4. The frequency response plots and the maximum magnitude and phase error plots of these s-domain models are generated using MATLAB software. In this section RC circuits of these s-domain models are created using partial fraction expansion formula given in Eqn. 9 and the results verified using OrCAD Capture CIS circuit simulator.

4.1. RC (RESISTOR CAPACITOR) CIRCUIT MODEL

The integer order function of FOD for the FB $[\omega_L \ \omega_H]$ rad/s is converted into partial fraction expansion form as follows [39]:

$$G(s) = A_P + \sum_{i=1}^{n} \left(\frac{sA_i}{(s+p_i)} \right) \quad (9)$$

The objective here is to develop an RC model of the FOD, analogous to the circuit of Fig. 19. The circuit is having one resistor and cascaded RC sets connected in parallel [39]. The RC sets count is dependent upon the number of poles of the integer order function. The resultant admittance of the circuit is [39]

$$Y(j\omega) = \frac{1}{R_p} + \sum_{i=1}^{n} \left(\frac{\frac{j\omega}{R_i}}{\left(j\omega + \frac{1}{R_i C_i} \right)} \right) \quad (10)$$

Comparing (9) and (10),

$$\frac{1}{R_p} = A_p \ , \ \frac{1}{R_i} = A_i \ , \ \frac{1}{R_i C_i} = p_i \quad (11)$$

Fig. 19 becomes the equivalent circuit of FOD.
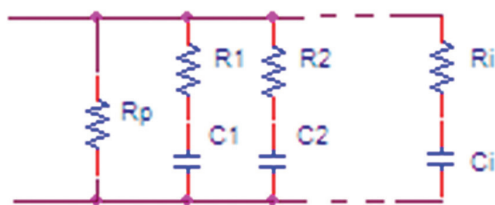
Fig. 19. RC circuit model

4.2. SCALING

Once an RC model of FOD is generated in one FB, the conventional method used to generate the RC model for the same FOD in another FB was to start from scratch i.e. first develop the integer order approximation in the desired FB and then find the values of R & C. But scaling is a technique in which this repetition of procedure is not required. Directly from the RC model of FOD first developed in the chosen FB, the models in other bands can be obtained as explained in this section. In case if it is desired to change only the magnitude of FOD and not the FB, magnitude scaling is also presented here. There are three types of scaling, namely: magnitude scaling, frequency scaling and magnitude-frequency scaling as given in Table 7.

Table 7. Scaling parameters

Scaling	Magnitude Scaling	Frequency Scaling	Magnitude-Frequency Scaling
Scale factor	m	k	a, b
New Scaled values	$[R'=R/m,$ $C'=mC]$	$[R'=R,$ $C'=C/k]$	$[R'=aR,$ $C'=C/(ab)]$
Remark	To shift magnitude, plot up/down	To shift magnitude and phase plots right/left	To simultaneously shift magnitude plot up/down and phase plot right/left

4.3. ONE-TENTH DIFFERENTIATOR $S^{0.1}$

The first example considered is a one-tenth differentiator $s^{0.1}$. Matsuda method is used to obtain the approximated integer order model given as

$$G_{0.1_{Matsuda}}(s) =$$
$$\frac{3.647s^4+2.049e5s^3+6.58e8s^2+1.575e11s+1.995e12}{s^4+7.891e4s^3+3.298e8s^2+1.027e11s+1.828e12} \quad (12)$$

The frequency range is set as 10^1 to 10^5 rad/s. For Matsuda based AIO transfer function nine frequency points are chosen within this range including the end frequencies. Hence the set of frequencies are [(10, 31.62, 100, 316.22, 1000, 3162.28, 10000, 31622.8, 100000)]. Eqn. 12 is transformed into partial fraction expansion form first and then the passive elements of the circuit are obtained using Eqn. 11.

The values for Matsuda approximated models are:

R_p=0.9163Ω;

R_1=0.9273 Ω; R_2=1.7050 Ω; R_3=2.2232 Ω; R_4=2.2676 Ω;

C_1=0.0144 mF; C_2=0.1440 mF; C_3=1.4000 mF; C_4=23.300 mF

All the values of R and C are positive.

These RC values are used to plot the frequency response of one-tenth differentiator $s^{0.1}$. The results obtained using OrCAD Capture CIS simulator is shown in Fig. 20. It is seen that the plot exhibits 2 dB/dec rise and the phase is approximately 9 deg as desired in the FB $[10^1 \ 10^4]$ rad/s.
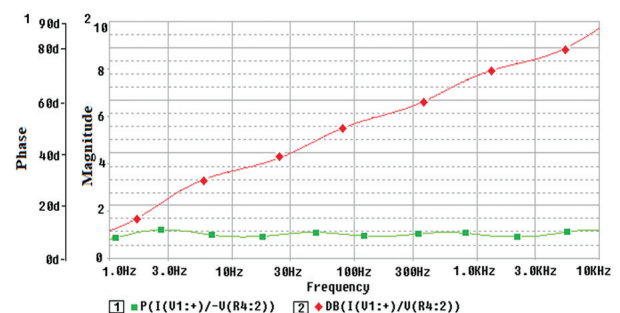
Fig. 20. Bode plot of one-tenth differentiator $s^{0.1}$ in the FB $[10^1 \ 10^4]$ obtained using RC values based on Matsuda method

In this example, frequency scaling is demonstrated on Eqn. (12) by changing the FBs. It has been mentioned earlier in Section 4.2 that, in case of frequency scaling only the capacitance values change. The scaling

factor 'k' is the frequency value by which the FB is to be changed. All the capacitances in the circuit are divided by 'k' to obtain the desired response.

Thus the new values of capacitances for only frequency shift are given as

$$C' = C \times \frac{1}{k} \; ; \; C' \text{ is new scaled capacitance} \quad (13)$$

Now, choosing $k=10$, the scaled capacitances obtained for one-tenth differentiator $s^{0.1}$ in the FB [10^2 10^5] are $C_1'=1.4475$ μF, $C_2'=0.0144$ mF, $C_3'=0.14$ mF and $C_4'=2.33$mF.

Similarly choosing $k = 10^3, 10^6, 10^9, 10^{12}$ and 10^{15}, the scaled parameter is derived for the FBs [10^4 10^7],[10^7 10^{10}], [10^{10} 10^{13}], [10^{13} 10^{16}] and [10^{16} 10^{19}] respectively.

Simulations with scaled capacitances for one-tenth differentiator $s^{0.1}$ are performed and it was observed that the frequency response plots were in correspondence to the frequency response plots of ideal one-tenth differentiator in the subsequent FBs of three-decade widths.
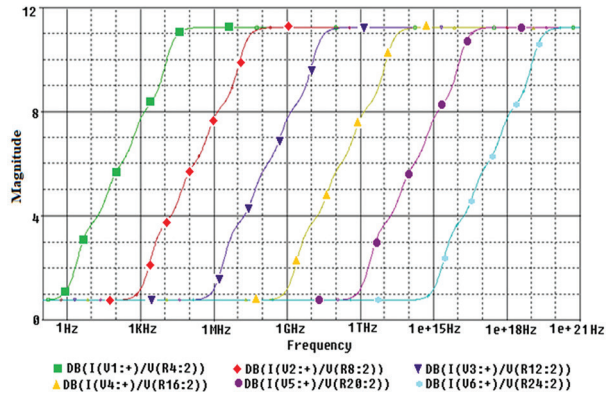
Fig. 21. Magnitude plots of Matsuda method based one-tenth differentiator $s^{0.1}$ for different FBs obtained by scaling of capacitances in the FB of interest

Figures 21 and 22 show magnitude and phase plots of one-tenth differentiator $s^{0.1}$ for different FBs [10^1 10^4], [10^4 10^7], [10^7 10^{10}], [10^{10} 10^{13}], [10^{13} 10^{16}] and [10^{16} 10^{19}] of 3 decades each. The total span of frequency is from 10^1 to 10^{19}, obtained by scaling of capacitances.

From Fig. 21, it is observed that the responses of $s^{0.1}$ differentiator obtained by scaling the capacitances in different FBs, match with their ideal responses in the FB of interest (i.e. for three decades). In each case the slope of the magnitude plot is 2dB/dec (as desired for a $s^{0.1}$ differentiator). It is further observed that there is no change in the magnitude when the FBs change. For each FB, the phase plots are shown in Fig. 22 (a-f).

It is again clear that the phase is approximately 9° (as desired for a $s^{0.1}$ differentiator) in the region of interest for the whole range with a maximum error of 1.8° and 0.8° in the ranges [10^1 10^4] and [10^2 10^4] rad/s respectively in each plot. Separate subplots have been purposefully shown so as to validate the results.

(a)

(b)

(c)

(d)

(e)

(f)
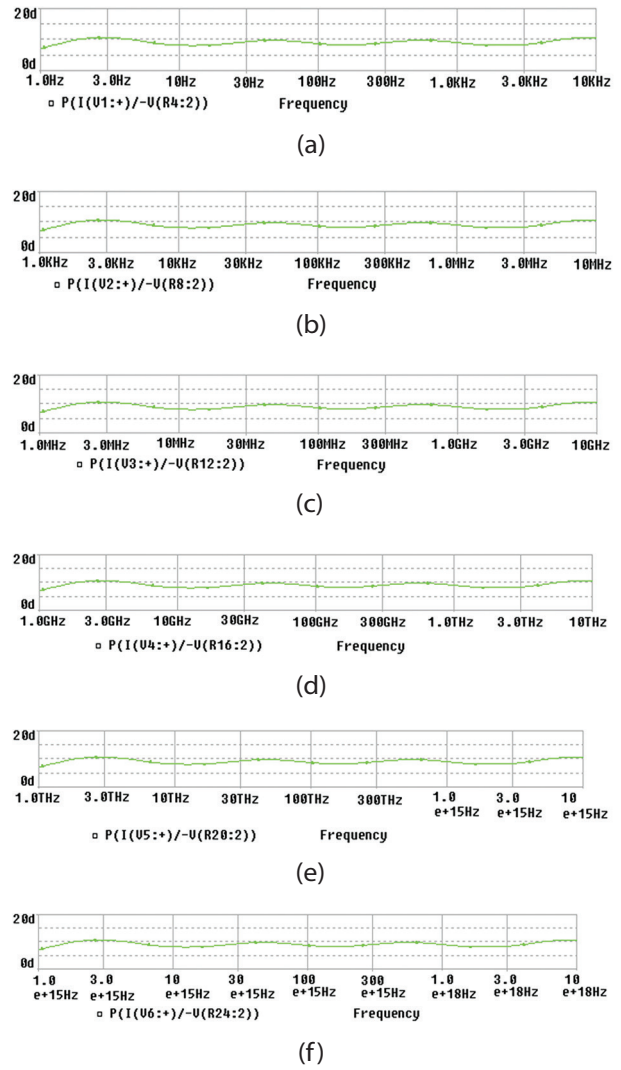
Fig. 22. (a)-(f). Phase plots of Matsuda method based one-tenth differentiator s^α (α=0.1) for different FBs [10^1 10^4], [10^4 10^7], [10^7 10^{10}], [10^{10} 10^{13}], [10^{13} 10^{16}] and [10^{16} 10^{19}] obtained by scaling of capacitances

4.4. SEVEN-TENTH DIFFERENTIATOR $s^{0.7}$

The Matsuda method is used to develop integer order approximations of $s^{0.7}$ in the FB [10^{-2} 10^2]. The approximation is given in Eqn. 14.

$$G_{0.7\_Matsuda}(s) = \frac{98.22s^4+2287s^3+3380s^2+349.3s+0.9996}{s^4+349.4s^3+3381s^2+2287s+98.2} \quad (14)$$

Eqn (14) is then transformed into partial fraction expansion form. Since the order of the approximation is 4, the number of circuit elements required as per Fig. 19 is nine (five resistances and four capacitances).

The values of the circuit elements obtained for Matsuda based AIO transfer functions are:

R_p=98.0392 Ω;

R_1=10.6mΩ; R_2=298.5m Ω; R_3=1.9869 Ω; R_4=11.1859 Ω;

C_1=277.7 mF; C_2=363.7 mF; C_3=738.2 mF; C_4=1.9393 mF

Using these RC values, the circuit is simulated with input voltage as 1V ac. The magnitude and phase plots

of seven-tenth differentiator $s^{0.7}$ is shown in Fig. 23. It is observed that the magnitude and phase values as obtained from the plot for all the frequency points in the chosen FB are very close to their corresponding ideal values in the whole FB.
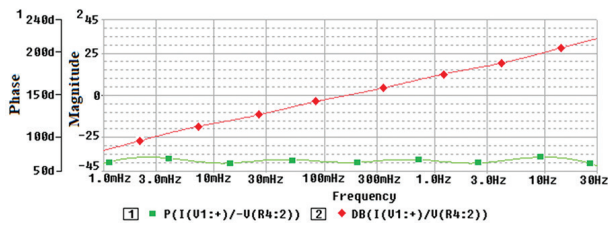
Fig. 23. Bode plot of seven-tenth differentiator $s^{0.7}$ in the FB [10^{-2} 10^2] obtained using RC values based on Matsuda method

The analysis for magnitude scaling is performed on the Matsuda model.

Now, if it is desired to change the magnitude (gain) of the FOD, magnitude scaling is applied. The scaling factor 'm' depends upon the desired change in magnitude. For an 'A' dB rise or fall in magnitude, the scaling factor is obtained as follows:

$$20 \log (m) = \pm A \qquad (15)$$

$$\therefore \ m = 10^{\pm \frac{A}{20}} \qquad (16)$$

Correspondingly all resistances are divided by factor 'm' and all capacitances are multiplied by factor 'm'.

Thus, new values of resistances and capacitances for magnitude shift are given as

$$\begin{aligned} R' &= R \times 1/m \ ; \ R' \ is \ new \ scaled \ resistance \\ C' &= C \times m \ ; \ C' \ is \ new \ scaled \ capacitance \end{aligned} \qquad (17)$$

The following two cases are considered for simulations on Matsuda approximated seven-tenth differentiator:

Case 1: 14 dB rise in magnitude

The scaling factor 'm' is calculated as 5.01187. The scaled values of resistances and capacitances are

Rp=19.56 Ω;
R_1=2.1149 mΩ; R_2=59.5586 mΩ; R_3=396.439 mΩ; R_4=.2318 Ω;
C_1=1.3917 F; C_2=1.8228 F; C_3=3.6997 F; C_4=1.7195 F

Case 2: 25 dB fall in magnitude

The scaling factor 'm' is calculated as 0.056234. The scaled values of resistances and capacitances are

R_p=174.34 KΩ;
R_1=188.84 mΩ; R_2=5.3081 Ω; R_3=35.33 Ω; R_4=198.91 Ω;
C_1=15.616 mF; C_2=20.45 mF; C_3=41.51 mF; C_4=109.054 mF

It can be seen that, all the values of R and C are positive.

Figure 24 shows the frequency response plot of seventh-tenth differentiator for different two different scaling factors. It can be seen that the magnitude plot is shifted up by 14 dB and down by 25 dB in the entire FB for Case 1 (red line with diamond shapes) and Case 2 (blue line with triangle shapes) respectively as desired. There is no change in the phase plots.
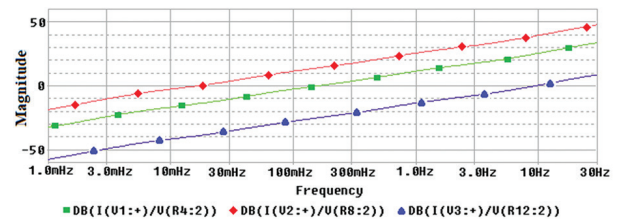
Fig. 24. Magnitude plots of Matsuda method based seven-tenth differentiator $s^{0.7}$ for different scaling factors

Similar simulations were performed for other FODs of order ($\alpha \in$([±0.1:±0.1:±0.9] and ±1/4, ±3/4)) (models presented in Table 1) with all RC elements having positive values.

5. CONCLUSION

In this paper, we have proposed s-domain stable models of f-o operator s^α developed using continued fraction expansion technique, popularly known as Matsuda method. The findings of the parameter sensitivity analysis are as follows: the parameter of importance is n, the number of frequency points within the FB of interest. It is observed that the selection of 'n' is directly proportional to the order of the approximated integer order transfer function and that the approximation is non-causal for odd values of n in case of FOD. A detailed frequency analysis is performed and it is seen that for the models proposed in our work, the error is less. Also, these models are most suitable for linear phase circuits as the phase response is almost flat in desired FB. In the Matsuda approximation method, if the number of frequency points chosen is $n \geq 13$, the phase response shows linear behaviour throughout the desired FB. An important point worth mentioning here is that the order of the approximated transfer function does not depend on the order of the fractional operator α. For the proposed model's direct realization in hardware is possible for f-o control purposes as the order is less and accuracy is high. In order to validate the proposed models so that they can be used for realization purposes, a structure with passive elements is designed and results of one tenth and seven tenth differentiator presented. Similar results were found for other FODs of order $\alpha(\alpha \in$([±0.1:±0.1:±0.9] and ±1/4, ±3/4)) (models presented in Table 1) with all RC elements having positive values. This shows that negative impedance converter is not required and also inductors, which would actually make the system bulky have not been used in circuit realization. This reduces the complexity of hardware realization. Another advantage of this design procedure is that there is only one junction other than reference junction. The scaling relations of R and C have been developed for smooth transition from one FB to another. Simulations were performed with scaled

parameters and it was found that the magnitude and phase response matched *20α dB/decade and 90α degrees* respectively.

6. REFERENCES

[1] X. Cui, D. Xue, F. Pan, "A fractional SVIR-B epidemic model for Cholera with imperfect vaccination and saturated treatment", The European Physics Journal Plus, Vol. 137, No. 1361, 2022.

[2] H. Sun, A. Chang, Y. Zhang, W. Chen, "A Review on Variable-Order Fractional Differential Equations: Mathematical Foundations, Physical Models, Numerical Methods and Applications", Fractional Calculus and Applied Analysis, Vol. 22, 2019, pp. 27-59.

[3] Y. Wei, Y. Chen, Y. Wei, X. Zhao, "Lyapunov stability analysis for nonlinear nabla tempered fractional order systems", Asian Journal of Control, Vol. 25, No. 4, 2023, pp. 3057-3066.

[4] S. Yadav, D. Kumar, J. Singh, D. Baleanu, "Analysis and dynamics of fractional order Covid-19 model with memory effect", Results in Physics, Vol. 24, 2021, p. 104017.

[5] A. Boudaoui, Y. E. Moussa, Z. Hammouch, S. Ullah, "A fractional-order model describing the dynamics of the novel coronavirus (COVID-19) with nonsingular kernel", Chaos, Solitons & Fractals, Vol. 146, 2021, p. 110859.

[6] P. Veeresha, E. Ilhan, D. G. Prakasha, H. M. Baskonus, W. Gao, "Regarding on the fractional mathematical model of tumour invasion and metastasis", Computer Modeling in Engineering & Sciences, Vol. 127, No. 3, 2021, pp. 1013-1036.

[7] A. Atangana, D. Baleanu, "New fractional derivatives with nonlocal and non-singular kernel: theory and application to heat transfer model", Thermal Science, Vol. 20, No. 2, 2016, pp. 763-769.

[8] K. B. Oldham, J. Spanier, "The Fractional Calculus: Theory and Applications of Differentiation and Integration to Arbitrary Order", 1st Edition, Dover Publications Mineola New York, USA, 2006.

[9] H. Sun, Y. Zhang, D. Baleanu, W. Chen, Y. Chen, "A new collection of real world applications of fractional calculus in science and engineering", Communications in Nonlinear Science and Numerical Simulation, Vol. 64, 2018, pp. 213-231.

[10] I. Petráš, "Fractional-Order Nonlinear Systems: Modeling, Analysis and Simulation", 1st Edition, Springer Berlin Heidelberg, 2011.

[11] W. Zheng, Y. Luo, X. Wang, Y. Pi, Y. Chen, "Fractional order PIλDμ controller design for satisfying time and frequency domain specifications simultaneously", ISA Transactions, Vol. 68, 2017, pp. 212-222.

[12] E. Yumuk, M. Güzelkaya, İ. Eksin, "A robust fractional-order controller design with gain and phase margin specifications based on delayed Bode's ideal transfer function", Journal of the Franklin Institute, Vol. 359, No. 11, 2022, pp. 5341-5353.

[13] R. Shalaby, M. El-Hossainy, B. Abo-Zalam, T. A. Mahmoud, "Optimal fractional-order PID controller based on fractional-order actor-critic algorithm", Neural Computing and Applications, Vol. 35, 2023, pp. 2347-2380.

[14] A. Latif, S. M. S. Hussain, D. C. Das, T. S. Ustun, A. Iqbal, "A review on fractional order (FO) controllers' optimization for load frequency stabilization in power networks", Energy Reports, Vol. 7, 2021, pp. 4009-4021.

[15] Z. Wu, J. Viola, Y. Luo, Y. Chen, D. Li, "Robust fractional-order [proportional integral derivative] controller design with specification constraints: more flat phase idea", International Journal of Control, Vol. 97, 2024, pp. 111-129.

[16] A. Oustaloup, F. Levron, B. F. M. Nanot, "Frequency band complex noninteger differentiator: Characterization and synthesis", IEEE Transactions on Circuits and Systems I: Fundamental Theory and Applications, Vol. 47, 2000, pp. 25-39.

[17] D. Y. Xue, C. Zhao, Y. Q. Chen, "A modified approximation method of fractional order system", Proceedings of the IEEE International Conference on Mechatronics and Automation, Louyang, China, 25-28 June 2006, pp. 1043-1048.

[18] A. Charef, H. H. Sun, Y. Y. Tsao, B. Onaral, "Fractal system as represented by singularity function", IEEE Transactions on Automatic Control, Vol. 37, 1992, pp. 1465-1470.

[19] G. Carlson, C. Halijak, "Approximation of fractional capacitors $(1/s)^{1/n}$ by a regular Newton process", IEEE Transactions on Circuit Theory, Vol. 11, 1964, pp. 210-213.

[20] N. Shrivastava, P. Varshney, "Rational Approxima-tion of Fractional Order Systems Using Carlson Method", Proceedings of the International Confer-ence on Soft Computing Techniques and Imple-mentation, Faridabad, India, 8-10 October 2015, pp. 76-80.

[21] K. Matsuda, H. Fujii, "H(∞)-optimized wave-ab-sorbing control -Analytical and experimental re-sults", Journal of Guidance, Control & Dynamics, Vol. 16, 1993, pp. 1146-1153.

[22] B. M. Vinagre, I. Podlubny, A. Hernandez, V. Feliu, "Some approximations of fractional order opera-tors used in control theory and applications", Jour-nal of Fractional Calculus and Applied Physics, Vol. 3, 2000, pp. 231-248.

[23] G. Maione, "On the Laguerre Rational Approxima-tion to Fractional Discrete Derivative and Integral Operators", IEEE Transactions on Automatic Con-trol, Vol. 58, No. 6, 2013, pp. 1579-1585.

[24] G. Maione, R. Caponetto, A. Pisano, "Optimization of zero-pole interlacing for indirect discrete ap-proximations of noninteger order operators", In-ternational Journal of Computers and Mathemat-ics with Applications, Vol. 66, 2013, pp. 746-754.

[25] J. D. Colín-Cervantes, C. Sanchez-Lopez, R. Ochoa-Montiel, D. Torres-Muñoz, C. M. Hernández-Mejía, L. A. Sánchez-Gaspariano, H. G. González-Hernán-dez, "Rational Approximations of Arbitrary Order: A Survey", Fractal and Fractional, Vol. 5, No. 4, 2021, p. 267.

[26] C. Sánchez-López, "An experimental synthesis methodology of fractional-order chaotic attrac-tors", Nonlinear Dynamics, Vol. 100, 2020, pp. 3907-3923.

[27] C. Sánchez-López, V. H. Carbajal-Gómez, M. A. Carrasco-Aguilar, I. Carro-Pérez, "Fractional-Order Memristor Emulator Circuits", Complexity, Vol. 2018, No. 1, 2018, p. 2806976.

[28] I. Podlubny, "Fractional-order systems and PIλDμ-controllers", IEEE Transactions on Automatic Con-trol, Vol. 44, 1999, pp. 208-214.

[29] C. Muñiz-Montero, L. V. García-Jiménez, L. A. Sánchez-Gaspariano, C. Sánchez-López, V. R. González-Díaz, E. Tlelo-Cuautle, "New alternatives for analog implementation of fractional-order integrators, differentiators and PID controllers based on integer-order integrators", Nonlinear Dynamics, Vol. 90, 2017, pp. 241-256.

[30] H. F. Raynaud, A. Zergaïnoh, "State-space repre-sentation for fractional order controllers", Auto-matica, Vol. 36, No. 4, 2000, pp. 1017-1021.

[31] C. A. Monje, B. M. Vinagre, A. J. Calderon, V. Feliu, Y. Q. Chen, "Auto-tuning of fractional lead-lag com-pensators", Proceedings of the 16th IFAC World Congress, Prague, Czech Republic, 4-8 July 2005, pp. 319-324.

[32] S. Kapoulea, C. Psychalinos, A. S. Elwakil, "Double exponent fractional-order filters: Approximation methods and realization", Circuits, Systems, and Signal Processing, Vol. 40, 2021, pp. 993-1004.

[33] S. Kapoulea, C. Psychalinos, A. S. Elwakil, "Power law filters: A new class of fractional-order filters without a fractional-order Laplacian operator", AEU - International Journal of Electronics and Communications, Vol. 129, 2021, p. 153537.

[34] D. Mondal, K. Biswas, "Performance study of frac-tional order integrator using single component fractional order element", IET Circuit, Devices and Systems, Vol. 5, No. 4, 2011, pp. 334-342.

[35] L. Dorcak, J. Valsa, E. Gonzalez, J. Terpak, I. Petras, "Analogue Realization of Fractional-Order Dy-namical System", Entropy, Vol. 15, No. 10, 2013, pp. 4199-4214.

[36] I. Podlubny, I. Petras, B. M. Vinagre, P. O'Leary, L. Dorcak, "Analogue Realization of Fractional-Order Controllers", Nonlinear Dynamics, Vol. 29, 2002, pp. 281-296.

[37] A. S. Elwakil, "Fractional-order circuits and sys-tems: An emerging interdisciplinary research area", IEEE Circuits and Systems Magazine, Vol. 10, No. 4, 2010, pp. 40-50.

[38] G. Radwan, A. Shamim, K. N. Salama, "Theory of fractional order elements based on impedance matching networks", IEEE Microwave and Wireless Components Letters, Vol. 21, No. 3, 2011, pp. 120-122.

[39] A. Charef, "Analogue realisation of fractional-order integrator, differentiator and fractional PIλDμ con-

troller", IEE Proceedings - Control Theory and Applications, Vol. 153, No. 6, 2006, pp. 714-720.

[40] D. Sierociuk, I. Podlubny, I. Petras, "Experimental Evidence of Variable-Order Behaviour of Ladders and Nested Ladders", IEEE Transactions on Control Systems Technology, Vol. 21, No. 2, 2013, pp. 459-466.

[41] M. A. Valencia-Ponce, P. R. Castañeda-Aviña, E. Tlelo-Cuautle, V. H. Carbajal-Gómez, V. R. González-Díaz, Y. Sandoval-Ibarra, J. Nuñez-Perez, "CMOS OTA-Based Filters for Designing Fractional-Order Chaotic Oscillators", Fractal and Fractional, Vol. 5, No. 3, 2021, p. 122.

[42] D. Patrinos, G. Tsirmpas, P. Bertsias, C. Psychalinos, A. S. Elwakil, "Implementation and Experimental Verification of Resistorless Fractional-Order Basic Filters", Electronics, Vol. 11, No. 23, 2022, p. 3988.

[43] B. T. Krishna, "Recent Developments on the Realization of Fractance Device", Fractional Calculus and Applied Analysis, Vol. 24, 2021, pp. 1831-1852.

[44] G. Tsirimokou, A. Kartci, J. Koton, N. Herencsar, C. Psychalinos, "Comparative Study of Discrete Component Realizations of Fractional-Order Capacitor and Inductor Active Emulators", Journal of Circuits, Systems and Computers, Vol. 27, No. 11, 2018, p. 1850170.

[45] M. F. Tolba, A. M. AbdelAty, N. S. Soliman, L. A. Said, A. H. Madian, A. T. Azar, A. G. Radwan, "FPGA implementation of two fractional order chaotic systems", AEU - International Journal of Electronics and Communications, Vol. 78, 2017, pp. 162-172.

[46] S. M. Mohamed, W. S. Sayed, L. A. Said, A. G. Radwan, "Reconfigurable FPGA Realization of Fractional-Order Chaotic Systems", IEEE Access, Vol. 9, 2021, pp. 89376-89389.

[47] A. Silva-Juárez, E. Tlelo-Cuautle, L. G. Fraga, R. Li, "FPAA-based implementation of fractional-order chaotic oscillators using first-order active filter blocks", Journal of Advanced Research, Vol. 25, 2020, pp. 77-85.